

journal of MEMBRANE SCIENCE

Journal of Membrane Science 306 (2007) 277-286

www.elsevier.com/locate/memsci

# Assessing feasibility of polyarylate—clay nanocomposites towards improvement of gas selectivity

Yogesh S. Bhole, Santosh D. Wanjale, Ulhas K. Kharul\*, Jyoti P. Jog

Polymer Science and Engineering Division, National Chemical Laboratory, Dr. Homi Bhabha Road, Pune 411008, India

Received 15 June 2007; received in revised form 8 August 2007; accepted 2 September 2007

Available online 7 September 2007

#### **Abstract**

Polymer–clay nanocomposites are well known to reduce the penetrant permeability by following tortuous path. Effects of such reduction in gas permeability on variation in selectivity of nanocomposites prepared using a high permeability polymer were examined. The polyarylate: poly(tetramethylbisphenolA-iso/terephthalate) that exhibits high permeability and moderate selectivity was chosen for making nanocomposites with two organically modified clays (Cloisite 6A and 10A) by solution intercalation method. The nanocomposite formation for various clay loadings (3, 5 and 7% w/w) in polyarylate was ascertained by change in physical properties (X-ray diffraction, DMA, TEM). Behavior of solution viscosity and nanocomposite density indicated existence of polymer–clay layer interactions. As anticipated, though the gas permeability of pure gases, viz., He, N<sub>2</sub>, CH<sub>4</sub> and CO<sub>2</sub> exhibited decrease, it was not monotonous. This decrease was more for larger gases (N<sub>2</sub>, CH<sub>4</sub> and CO<sub>2</sub>) in comparison to the decrease for smaller gas (He) permeability. This led to a decrease in CO<sub>2</sub>/N<sub>2</sub> and CO<sub>2</sub>/CH<sub>4</sub> selectivities and increase in He/CO<sub>2</sub> selectivity; while He/CH<sub>4</sub> selectivity was increased substantially at 7% clay loading. This variation indicated feasibility of nanocomposites formation as a tool for improving selectivity of certain gas pairs.

© 2007 Elsevier B.V. All rights reserved.

Keywords: Nanocomposites; Gas permeation; Selectivity; Polyarylates; Solution intercalation

#### 1. Introduction

Layered silicates are widely used for preparation of nanocomposites. Permeation properties of these nanocomposites are known to be greatly different than that of pristine polymer. Due to impermeable nature of silicate layers, diffusing molecule has to follow the 'tortuous path', increasing diffusion path length leading to reduction in permeability of various molecules like water vapor in poly(vinyl alcohol) [1], poly(urethane urea) [2], polyimide [3], poly( $\varepsilon$ -caprolactone) [4]; oxygen permeability in case of polyimide [3,5] and poly(lactic acid) [6]; CO<sub>2</sub> permeability in polyimide [7], etc. The reduction in permeability by nanocomposite formation was mainly investigated in view of barrier property improvement. Studies on permeation of different gas molecules in same nanocomposites are also reported. These

include butyl rubber/vermiculite [8], LLDPE-montmorillonite [9], PP-clay nanocomposites [10], etc. These studies report marginal [8] to significant [10] variations in selectivity of certain gas pairs reported. On the other hand, addition of fumed silica in poly(1-trimethylsilyl-1-propyne) [11] and poly(4-methyl-2-pentyne) [12] led to improved gas permeation properties of the resulting nanocomposites.

In the case of PP-clay nanocomposite, reduction in He permeability was mainly diffusion controlled, while permeability of N<sub>2</sub> and O<sub>2</sub> was lowered by the reduction in both, solubility and diffusivity [10]. In butyl rubber/vermiculite nanocomposites, CO<sub>2</sub> sorption was found to be increased mainly due to the gas adsorption on vermiculite [8]. Improved transport properties in fumed silica–PTMSP nanocomposites was related to the increase of free volume in PTMSP beyond the solution-diffusion realm [11], while in case of fumed silica–PMP nanocomposites, nanometer-sized fumed silica particles disrupt packing of rigid, bulky PMP chains, thereby subtly increasing the free volume available for molecular transport [12]. A trade-off relationship while modifying permeation properties of polymers, i.e. an effort

<sup>\*</sup> Corresponding author. Tel.: +91 20 25902180; fax: +91 20 25902618. *E-mail addresses:* ys.bhole@ncl.res.in (Y.S. Bhole), sd.wanjale@ncl.res.in (S.D. Wanjale), uk.kharul@ncl.res.in (U.K. Kharul), jp.jog@ncl.res.in (J.P. Jog).

Table 1 Specifications of MMT 6A and 10A

Clay used	Ammonium cation	Modifier concentration (mequiv./100 g)	Basal spacing of as received clay (001) (nm)	Basal spacing of toluene treated clay (001) (nm)	Clay density (g cm <sup>-3</sup> )
Cloisite 6A	$(CH_3)_2(HT^a)_2N^+ \ (CH_3)_2(HT^a) (CH_2C_6H_5)N^+$	140	3.4	2.75	1.9
Cloisite 10A		125	2.0	1.91	1.71

<sup>&</sup>lt;sup>a</sup> T, tallow (65% C18, 30% C16, 5% C14), HT, hydrogenated tallow.

to increase gas permeability generally leads to reduced selectivity and vice versa [13], is well known.

Though nanocomposite formation generally leads to the reduction in permeability, this as a tool to improve selectivity may be promising by following the trade-off relationship. This aspect looks almost unaddressed in the literature and became the objective of the present work. The polymer with high permeability was purposely chosen to analyze feasibility of such trade-off relationship in improving selectivity. A glassy polyarylate: poly(tetramethylbisphenolA-iso/terephthalate) exhibits appreciable gas permeability [14] and good solvent solubility. By solvent intercalation, the nanocomposites with two different types of clay (MMT 6A and 10A, that differ in organic modifier) with varying clay loading were prepared to analyze physical and gas permeation properties of resulting nanocomposites.

#### 2. Experimental

## 2.1. Materials

2,6-Dimethylphenol and benzyltriethylammonium chloride (BTEAC) were procured from M/s. Fluka, Switzerland. Isophthalic acid (IPA) and terephthalic acid (TPA) were procured from M/s. Aldrich Chemicals, USA. Thionyl chloride, toluene and petroleum ether (LR grade) were obtained from M/s. S.D. Fine Chemicals, India. Organically modified montmorillonite (MMT) Cloisite 6A and 10A (specifications as given in Table 1) were supplied by Southern Clay Products, USA. 2,6-Dimethylphenol was purified by distillation, while other materials were used as received.

TetramethylbisphenolA was prepared by the acid catalyzed condensation of 2,6-dimethylphenol with acetone according to the procedure of Venkateswara et al. [15]. The dicarboxylic acids (IPA and TPA) were converted to their respective acid chlorides (IPC or TPC) by refluxing an acid in 4 mequiv. of thionyl chloride using *N*,*N*-dimethyl formamide as the catalyst. Obtained acid chlorides were purified by the recrystallization in dry petroleum ether. Chemical structures of monomers and the resulting polyarylate are given in Fig. 1.

The polyarylate: poly(tetramethylbisphenolA-iso/terephtha-late) (PA) was synthesized by controlled addition of CH<sub>2</sub>Cl<sub>2</sub> solution of IPC and TPC (2:8) in aqueous Na-salt solution of tetramethylbisphenolA containing phase transfer agent (BTEAC) by interfacial manner [14]. Obtained polymer was purified by reprecipitation of its CHCl<sub>3</sub> solution into methanol. Toluene treatment for each of these clay samples was done for removing excess organic modifier. The clay was stirred in

toluene (1% w/v) for 12 h, separated by filtration and dried at 60 °C for 24 h.

#### 2.2. Nanocomposite preparation

The solution intercalation approach was employed to prepare polyarylate-organoclay nanocomposites. Toluene was selected as a solvent, in which polyarylate (PA) showed good solubility and organically modified montmorillonite (10A and 6A) exhibited good dispersability. Three grams of PA and varying amount of vacuum dried (60 °C, 24 h) as received clay (3, 5 or 7 wt.% of the polymer) was added to 45 ml of toluene and stirred for 12 h. The obtained clear suspension was poured on to a flat glass surface, allowing solvent evaporation at an ambient temperature and dry conditions. The formed film was peeled off and kept under vacuum at 60 °C for a week in order to ensure complete removal of the residual solvent. These films were transparent in nature and no clay agglomeration could be seen. The nanocomposites based on 6A clay are abbreviated as PA-6A and that based on 10A clay are abbreviated as PA-10A, with suffix denoting the weight percent of clay loading as given in Table 2.

Poly(tetramethylbisphenolA-iso/terephthalate)

Fig. 1. The structure of monomers and polymer used.

Table 2
Physical properties of nanocomposites containing varying percent loading of 6A and 10A clay

Nanocomposite abbreviation	Clay used, its loading (wt.%)	$d_{\rm sp}^{\rm a}$ (Å)	$[\eta](dlg^{-1})$	$\rho  (\mathrm{g  cm^{-3}})$
PA <sub>0</sub>	_	6.01	0.37	1.103
PA-6A <sub>3</sub>	6A, 3	5.76	0.44	1.111
PA-6A <sub>5</sub>	6A, 5	5.89	0.46	1.124
PA-6A <sub>7</sub>	6A, 7	5.75	0.53	1.135
PA-10A <sub>3</sub>	10A, 3	5.75	0.52	1.127
PA-10A <sub>5</sub>	10A, 5	5.47	0.57	1.133
PA-10A <sub>7</sub>	10A, 7	5.75	0.61	1.144

<sup>&</sup>lt;sup>a</sup> d-Spacing corresponding to polymer amorphous hollow in XRD scan.

#### 2.3. Characterizations

The X-ray diffraction studies of nanocomposites in the film form, while that of clays in powder form (as received and toluene treated) were performed using Rigaku X-ray diffractometer ( $D_{\text{max}}$  2500) with Cu K $\alpha$  radiation and were as given in Figs. 2 and 5(a and b) for clays and nanocomposites, respectively. The basal spacing of clays was estimated from the (001) peak in the XRD pattern. The average d-spacing value  $(d_{sp})$ for the polymer peak (amorphous hollow) was calculated from the peak maxima using Bragg's equation. The scanning electron micrograph (S.E.M.) of clay in powder form (as received and toluene treated) and nanocomposites were recorded with Leica, stereoscan-440. The dispersability of intercalated clay particles in the nanocomposite matrix was evaluated by means of transmission electron microscope (TEM, Jeol-1200 EX instrument), operated at an accelerating voltage of 80 kV (Fig. 6). The TEM specimens were cut from 50 µm thick nanocomposite films using ultramicrotome equipped with a diamond knife. The TGA of clay (as received and toluene treated) was performed on Perkin-Elmer TGA-7 at 20 °C min<sup>-1</sup> under N<sub>2</sub> atmosphere from ambient to 700 °C. The dynamic mechanical analysis (DMA) was performed using Rheometrics DMTA III E, in the temperature range of ambient to 300 °C, at the frequency of  $10 \,\mathrm{rad}\,\mathrm{s}^{-1}$  and at 0.1% strain using a film specimen. The intrinsic viscosity  $[\eta]$  of polymer solutions containing clay was determined by graphical method at 35 °C using toluene as a solvent. The density  $(\rho)$  of nanocomposites in the film form was determined by flotation method using aqueous K<sub>2</sub>CO<sub>3</sub> solutions at 40 °C.

# 2.4. Permeability determination

The pure gas permeability measurements for He,  $N_2$ , CH<sub>4</sub> and CO<sub>2</sub> (used in the same sequence every time) were performed at 35 °C and at 10 atm upstream pressure using variable volume method, while maintaining the permeate side at ambient pressure. Measurements were repeated for three membrane samples prepared individually under identical conditions and results averaged (variation up to  $\pm 8\%$  from average value, depending on gas analyzed). The permeability and selectivity ( $\alpha$ , ratio of pure gas permeability) were as given in Table 3.

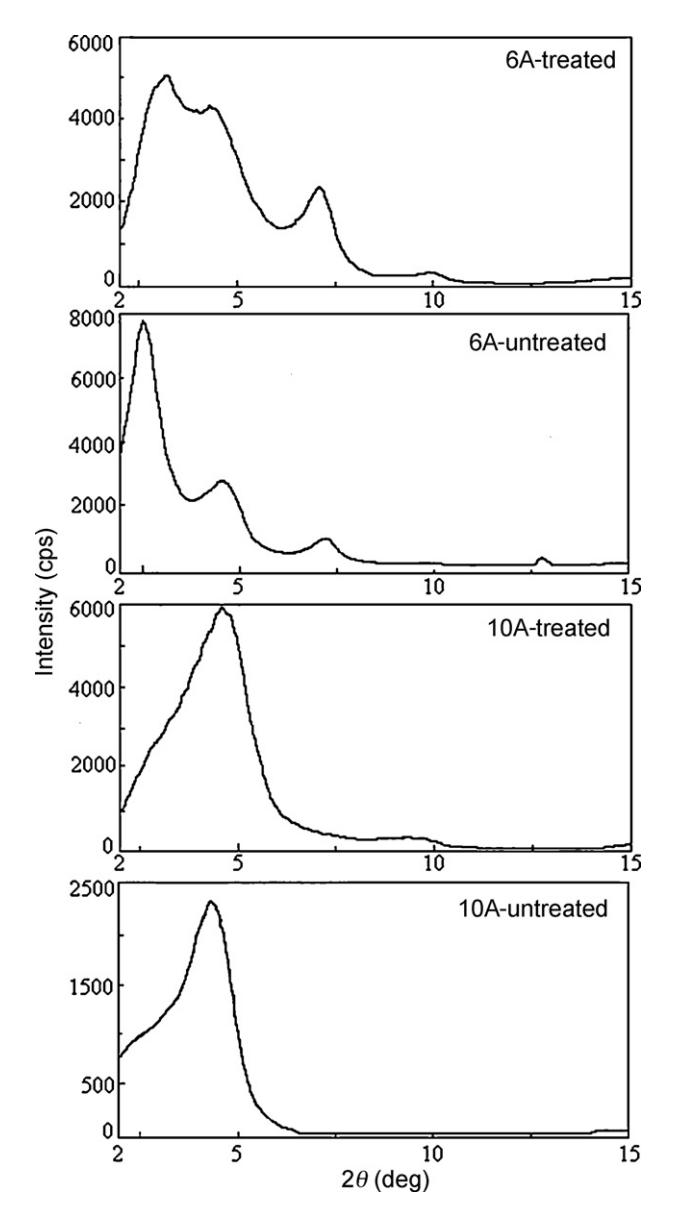


Fig. 2. Wide angle X-ray diffraction spectra for treated and untreated clays.

Table 3 Permeability coefficient  $(P)^a$  and selectivities  $(\alpha)^b$  for nanocomposites with different percent loading of clays

Gas	PA	6A clay			10A clay		
		3%	5%	7%	3%	5%	7%
Не	43.7	31.8	28.1	21.4	29.4	26.4	16.1
$N_2$	1.2	1.2	0.8	0.7	1.0	0.84	0.66
$CH_4$	1.04	0.93	0.85	0.3	0.75	0.67	0.30
$CO_2$	41.6	20	14.2	3.8	16.1	12.2	3.7
$\alpha(\text{He/N}_2)$	36.4	26.5	35.1	30.6	29.4	31.4	24.4
$\alpha(\text{He/CH}_4)$	42	34.2	33.1	71.3	39.2	39.4	53.7
$\alpha(\text{He/CO}_2)$	1.05	1.59	1.98	5.63	1.83	2.16	4.35
$\alpha(\text{CO}_2/\text{N}_2)$	34.7	16.7	17.8	5.4	16.1	14.5	5.6
$\alpha(\text{CO}_2/\text{CH}_4)$	40	21.5	16.7	12.7	21.5	18.2	12.3

 $<sup>^</sup>a$  Permeability expressed in Barrer (1 Barrer = 1  $\times$   $10^{-10}\,cm^3$  (STP)  $cm\,cm^{-2}\,s^{-1}\,cm\,Hg^{-1}).$ 

<sup>&</sup>lt;sup>b</sup> Ratio of pure gas permeability.

#### 3. Results and discussion

# 3.1. Characterization of clays

Organoclays (6A and 10A) are layered silicates where the organic modifier is introduced by ion exchange. Montmorillonite, one of the clay minerals used as polymer filler, is available as micron-size tactoids, consisting of several hundred individual platy particles (each plate-like layer is about 1 nm thick and from 50 nm to about 100 nm in lateral dimension) held together by electrostatic forces, with a gap of  $\sim$ 0.3 nm between two adjacent particles [16]. Xu et al. reported that common platy filler materials such as montmorillonite, saponite, synthetic mica, etc. are composed of stacked silicate layers of approximately 10-2000 nm in length and 1 nm in thickness [17]. Due to natural defects/charge heterogeneity on the clay plates, not all of the clay plates could be fully ion exchanged. Therefore, some of the organic surfactant could remain associated with the clay after ion exchange, but it would not be ionically bonded to the surface and remain only physically sorbed on to the surface. This excess surfactant (organic modifier) can be removed by solvent washes [18]. Fig. 2 presents the XRD scan of the as received and toluene treated clays. After toluene treatment, a decrease in d-spacing was observed in the case of 6A. The d-spacing was reduced from 3.44 to 2.75 nm. This indicated that the toluene treatment removed an excess organic modifier associated with the clay. For 10A clay, a marginal decrease of 0.1 nm in d-spacing was observed. The thermogravimetric analysis of toluene treated and as received clay (vacuum dried) showed that in the case of 6A clay, 3.63 wt.% loss of excess surfactant occurred, while it was 0.51% in the case of 10A clay at 400  $^{\circ}$ C. The S.E.M. images of both the clays (as received and after toluene treatment) are shown in Fig. 3. The agglomeration of clay particles was observed after toluene treatment followed by drying.

# 3.2. Formation of nanocomposite

The method of solution intercalation using toluene as a solvent was adopted in the present investigation. The solution intercalation is known to be one of the methods for preparing polymer-clay nanocomposites [19-21]. Though melt intercalation is a widely used method and is environmentally benign, polymer processing capability under melt condition becomes an essential criteria. This was not established for the present PA. Moreover, the objective of the present work was to analyze permeation properties of membranes. Thus, the method of solution intercalation was preferred over other methods of nanocomposite preparation. As stated in the previous section, TGA analysis of toluene treated and untreated clays showed that the excess modifier (unbound) was present only in smaller quantity. Thus as received clays (without toluene treatment but after vacuum drying) were used for the preparation of nanocomposites. The selection of solvent (toluene) was based on solubility of the polymer and well dispersabil-

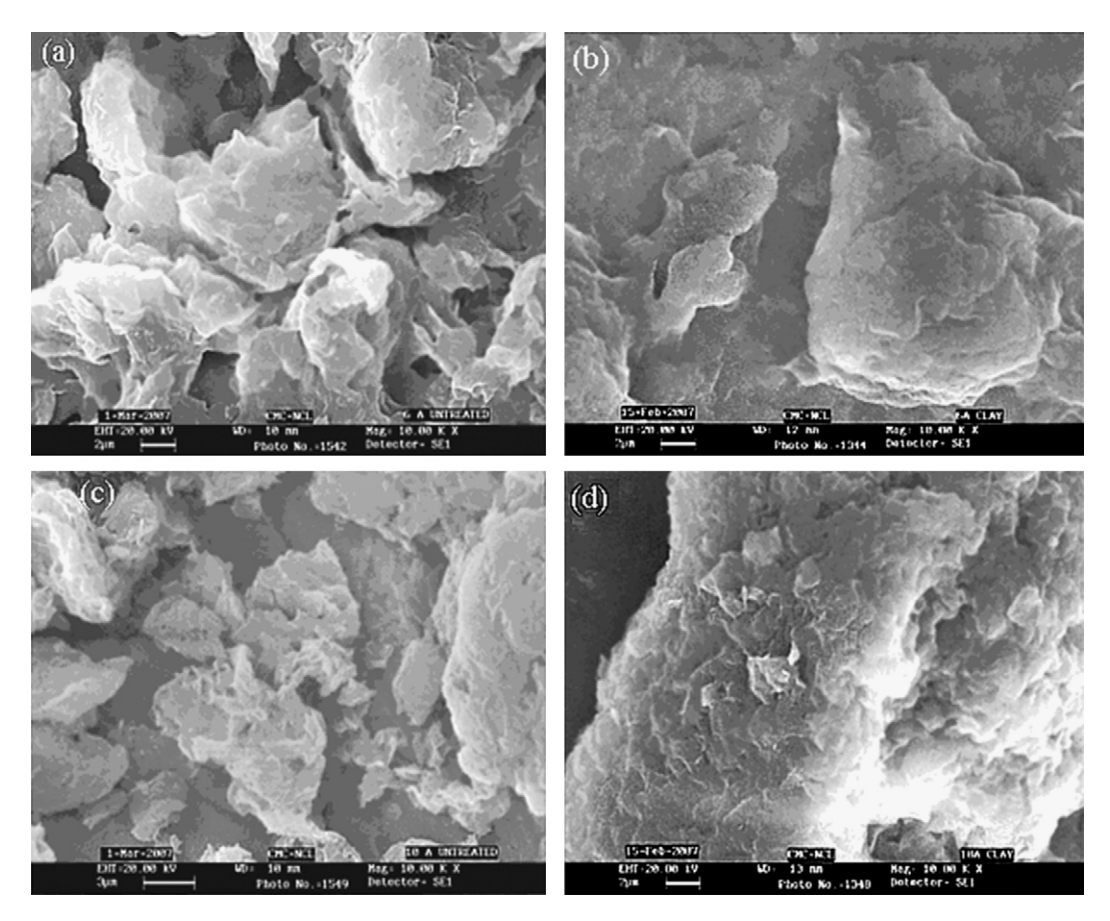


Fig. 3. S.E.M. of clay: (a) 6A-untreated, (b) 6A-treated, (c) 10A-untreated, (d) 10A-treated.

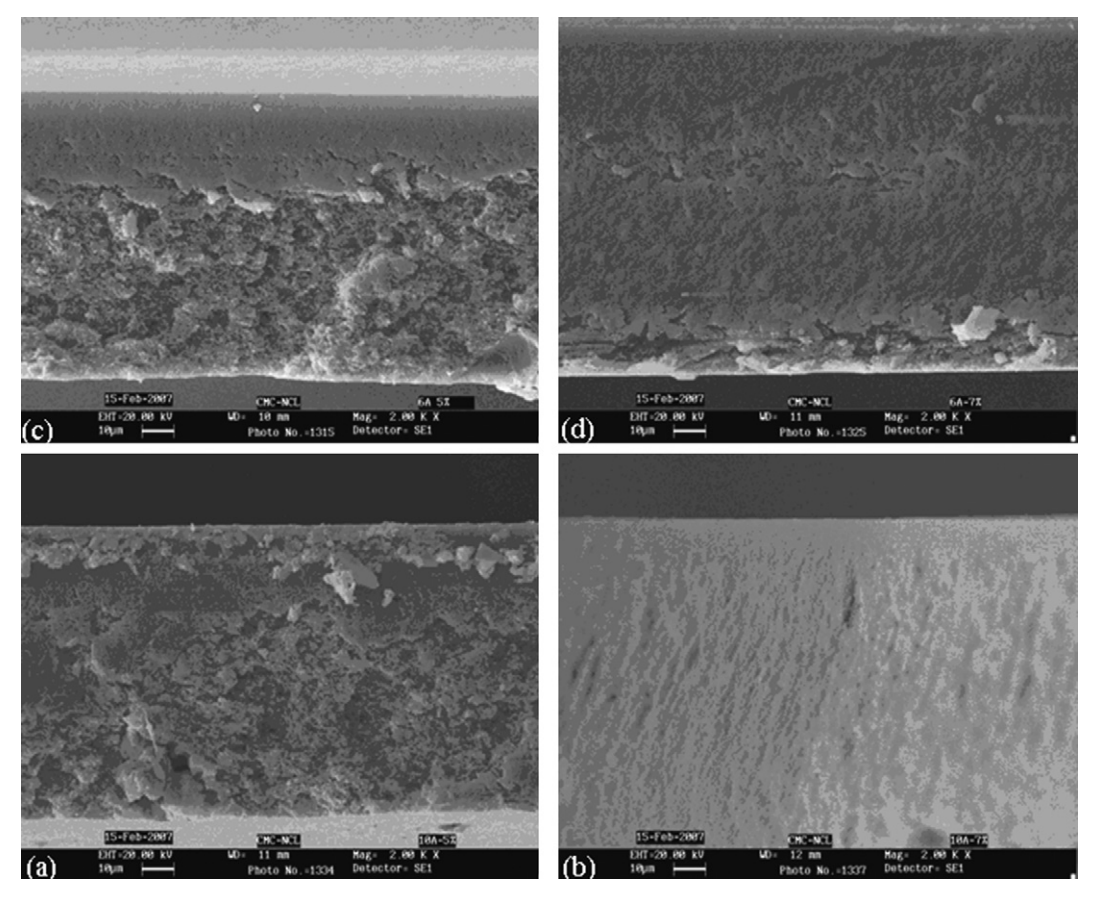


Fig. 4. S.E.M. of nanocomposites: (a)  $PA-10A_5$ , (b)  $PA-10A_7$ , (c)  $PA-6A_5$ , and (d)  $PA-6A_7$ .

ity of the clay particles. No agglomeration was observed when both the types of clay were suspended in toluene. It is said that high solubility of polymer and good dispersion of silicate are the primary criteria used in the solvent selection for solution intercalation [22]. Toluene was also reported to be a solvent for solution intercalation using silicate—clays (MMT) [19,21]. Manninen et al. [21] has reported that toluene was found to produce the finest clay (Cloisite 20A) suspension among various solvents examined. The S.E.M. images of 5 and 7% clay (of both the types) containing nanocomposites are given in Fig. 4, which did not indicate any clay agglomeration.

# 3.3. Characterization of nanocomposites

# 3.3.1. X-ray diffraction, TEM and DMA studies

Fig. 5a shows X-ray diffraction spectra for 6A clay based nanocomposites. As can be seen from Fig. 2, toluene treated 6A clay exhibited three well defined peaks with  $d_{001}$  peak having d-spacing of about 2.75 nm. However, in the case of nanocomposites, only one diffraction peak was observed at the higher d-spacing. Increase in the d-spacing was about 0.33, 0.37 and 0.13 nm for 3, 5 and 7% 6A-clay loading, respectively. This indicated that the intercalation of polymer resulted in a new set of diffraction planes. Increase in the d-spacing is known to result from disordered intercalated structure of nanocomposites [23,24].

Fig. 5b shows X-ray diffraction patterns for the 10A clay nanocomposites. A shift in  $2\theta$ -value to the lower angle indicating an increase in the d-spacing of clay was seen. This increase was about 0.37, 0.46 and 0.37 nm for the nanocomposites with 3, 5 and 7% 10A-clay loading, respectively. This confirmed the disordered intercalation of the polymeric chains inside the clay galleries. The  $d_{\rm sp}$  calculated for amorphous hollow responsible for polymer fraction of nanocomposite was found to be decreased in both the types of clays, supporting that polymer chains and clay in the formed nanocomposites exhibited some interactions, as also indicated by the increase in solution viscosity and the density (as elaborated in Section 3.3.2 below). The nanocomposite formation was also confirmed by the transmission electron micrograph (TEM) for both the types of clay loading in PA. Fig. 6 for nanocomposites with 5% clay loading with different magnifications shows better dispersion of silicate layers in 10A based nanocomposites than that in 6A based.

The dynamic mechanical analysis was carried out to study the effect of organically modified layered silicates on the glass transition (as indicated by  $\tan \delta$  peak temperature) and the sub- $T_{\rm g}$  transition temperatures of these nanocomposites. Temperature dependence of  $\tan \delta$  peak for the pristine polymer and the nanocomposites studied is presented in Fig. 7. The value of  $T_{\rm g}$  (maximum of the  $\tan \delta$  peak) was 271 °C for the pristine polymer, PA. As the percent clay loading increased, the  $T_{\rm g}$  was reduced to 263–255 °C in the case of 6A clay based nanocomposites and between 262 and 255 °C in the case of 10A clay based nanocom-

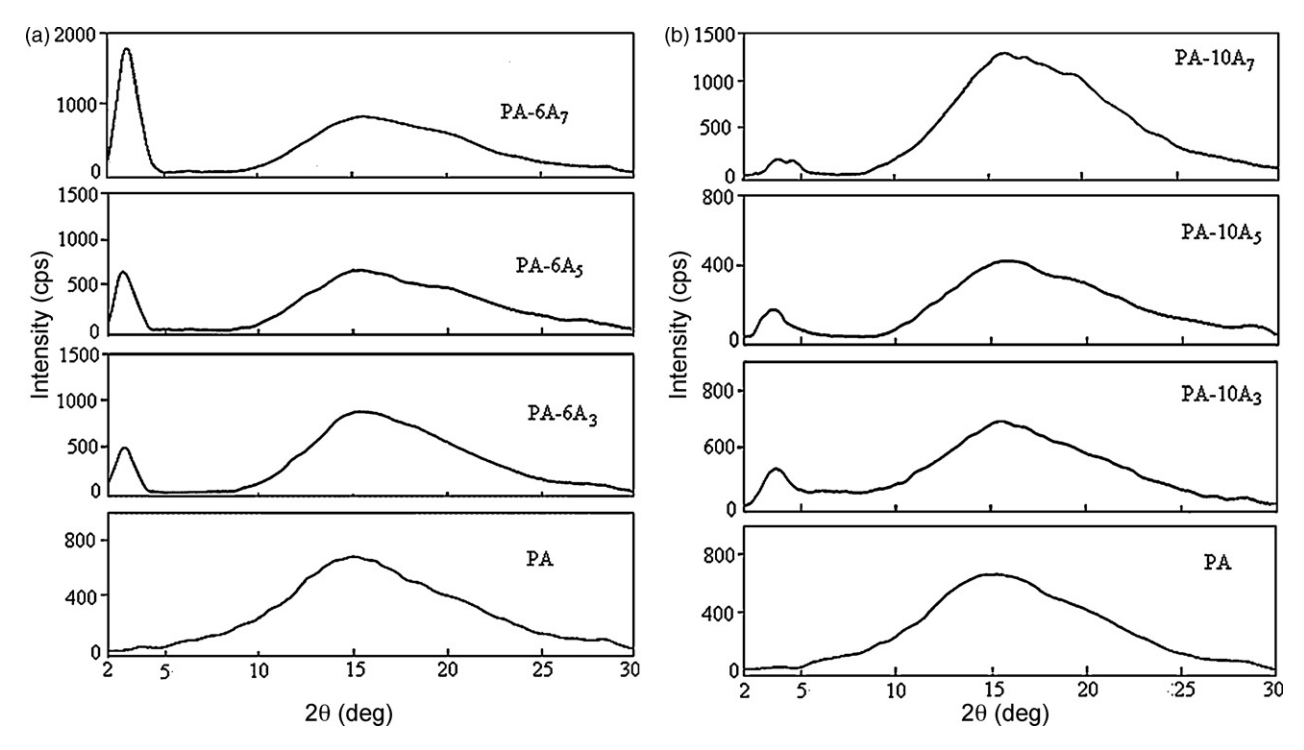


Fig. 5. (a) Wide angle X-ray diffraction spectra for PA and nanocomposites based on 6A clay. (b) Wide angle X-ray diffraction spectra for PA and nanocomposites based on 10A clay.

posites. Decrease in the  $T_{\rm g}$  followed the order of increasing clay loading for both types of nanocomposites. This lowering in  $T_{\rm g}$  could be attributed to the plasticization effect caused by organic modifier molecules of the layered silicates. There are reports that

the organic modifier of clay can lead to the decrease in glass transition temperature of polymer–clay nanocomposites [20,25,26]. In PVC–clay nanocomposites, ammonium compound of the clay served as a plasticizer by lowering the melt-compounding tem-

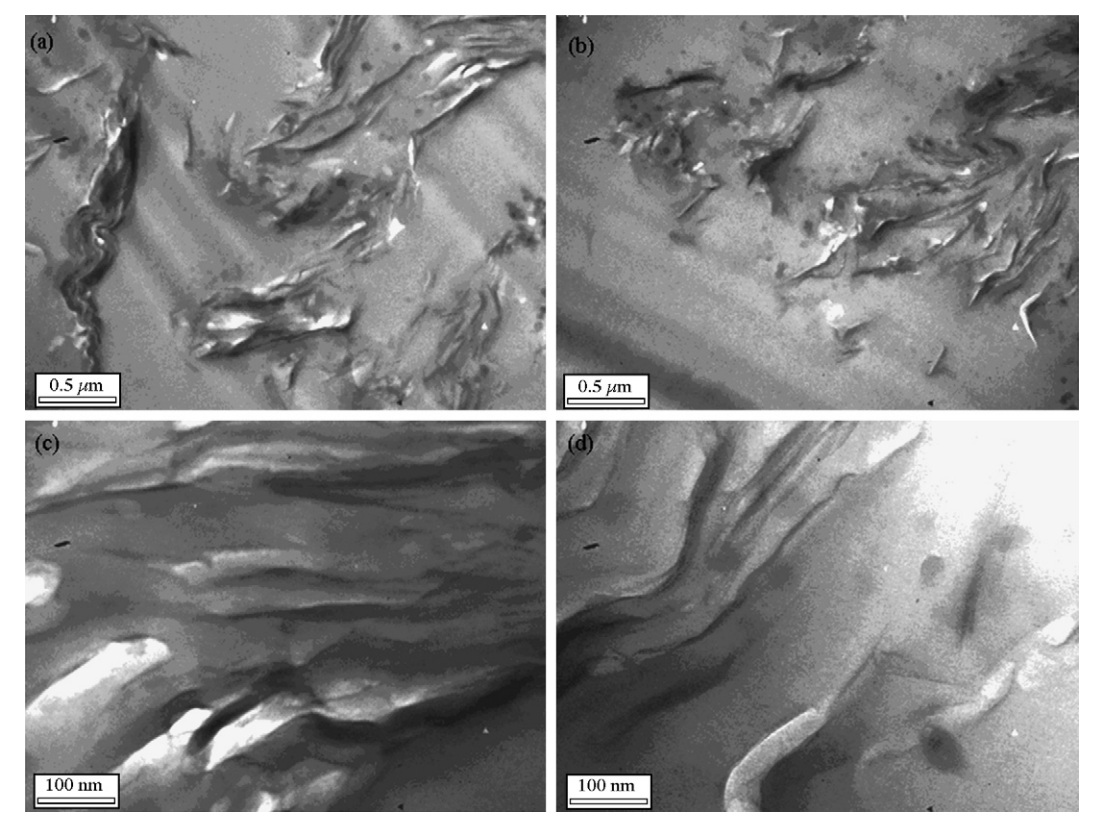


Fig. 6. TEM of nanocomposites: (a) PA-6A<sub>5</sub>, and (b) PA-10A<sub>5</sub> (low magnification). (c) PA-6A<sub>5</sub>, and (d) PA-10A<sub>5</sub> (with higher magnification).

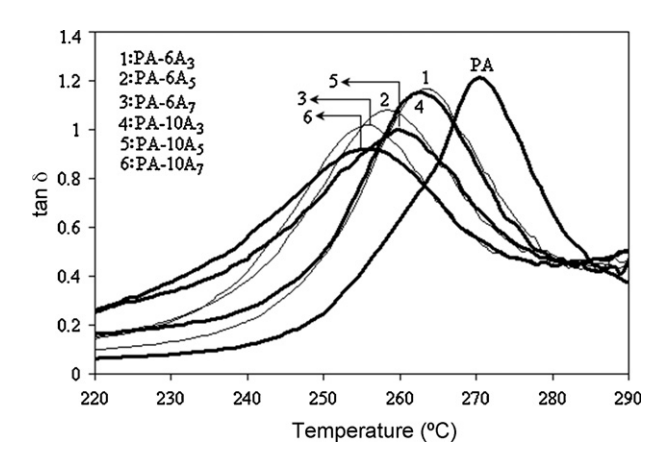


Fig. 7.  $\tan \delta$  curve by DMA of PA and nanocomposites.

perature of PVC [25]. In polyimide/clay nanocomposites, long alkyl (dodecyl) groups in the organophilic clays provided a significant plasticizing effect, thus resulting in a reduction in  $T_{\rm g}$  [20].

# 3.3.2. Solution viscosity and nanocomposite density

The intrinsic viscosity data for PA solutions containing different 10A and 6A clay content is summarized in Table 2. A linear increase in viscosity with increasing clay loading was observed for solutions containing both the types of clay. For a particular percent loading, an increase in viscosity was found to be higher in the case of 10A than that for 6A clay based solutions, indicating better interactions of 10A clay with the polymer chains than that of the 6A clay. Density of the nanocomposites determined by floatation method are given in Table 2. Density for both the types of nanocomposite increased with an increase in the loading content. For 10A based nanocomposites, the density was higher than that for 6A based nanocomposites for the same level of loading.

In the present case, clays contain organic modifier (ammonium cation) having different groups (Table 1). The modifier of 10A contains phenyl ring in the alkyl chain, while 6A does not contain phenyl ring. As a result, better interaction based dispersion of clay particles in wholly aromatic polyarylate PA could be anticipated with the 10A type of clay. It is said that in comparison to Cloisite 6A, the replacement of one hydrogenated tallow group by the benzyl group gives Cloisite 10A the proper hydrophobicity and compatibility with PBT, which in turn favors extensive intercalation [27]. It should be noted here that PBT also contains aromatic rings in its backbone. Observed variations in the density and solution viscosity of present nanocomposites based on 6A and 10A may have originated from this basic structural difference of the organic modifier.

#### 3.4. Permeation properties of nanocomposites

# 3.4.1. Effect on permeability

Gas permeability investigations of nanocomposites based on both types of clay was performed using pure gases viz. He,  $N_2$ ,  $CH_4$  and  $CO_2$  and the results are summarized in Table 3. For both the types of nanocomposites, an overall decrease in permeabil-

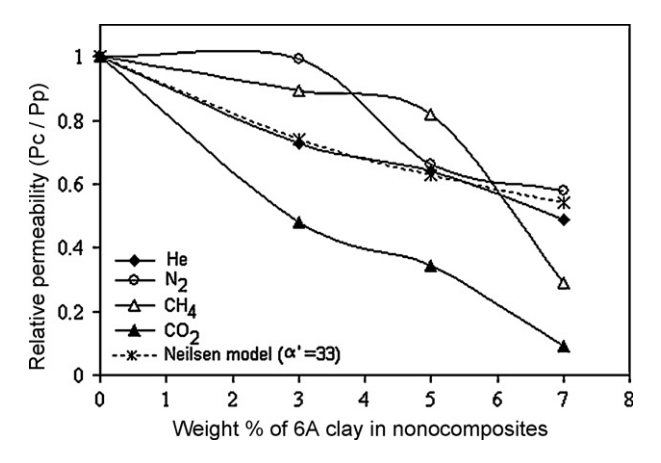


Fig. 8. Variation of relative permeability  $(P_c/P_p)$  with volume fraction  $(\phi_f)$  of 6A based nanocomposites.

ity for all gases was observed in comparison to that of pristine PA. This could be attributed to both, an increase in tortuous path length as well as to closer PA chain packing in nanocomposites, in comparison to the pristine polyarylate (as revealed by lowering in  $d_{\rm sp}$ ). It is known that platelet type morphology of the clay particles embedded in a polymer matrix increase diffusion path length by following a 'tortuous path', leading to the lowering in permeability [28,29]. Various polymer—clay nanocomposites exhibited a large decrease in permeability for different gases [8–10], as also observed in the present case.

The decrease in permeability was slightly more in the case of 10A based nanocomposites than in the case of 6A based nanocomposites at the same level of clay loading. This could be attributed to the lower available free volume in earlier cases at a particular loading level. This was indicated by (a) lowering in  $d_{\rm sp}$  of the polymer fraction in the nanocomposites (Table 2), as a result of better interaction of 10A clay with PA than that of 6A clay and (b) observed higher density and solution viscosity for 10A based nanocomposites than for their 6A based counterparts.

Variation in relative permeability ( $P_{\text{nanocomposite}}/P_{\text{PA}}$ ) with the volume fraction of clay loading were as presented in Figs. 8 and 9, for 6A and 10A clay based nanocomposites,

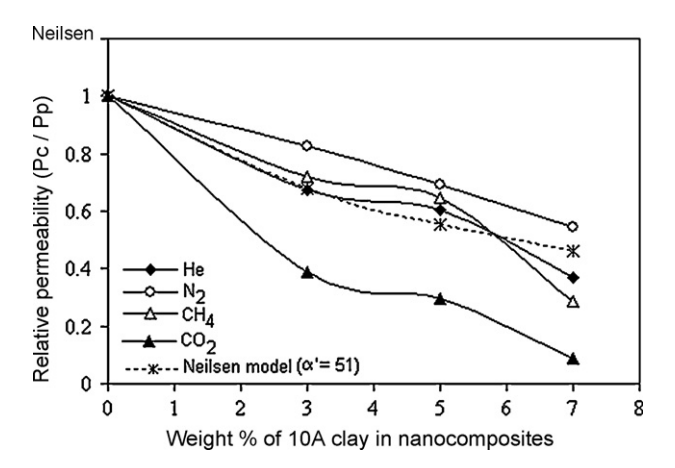


Fig. 9. Variation of relative permeability  $(P_c/P_p)$  with volume fraction  $(\phi_f)$  of 10A based nanocomposites.

respectively. This ratio decreased with increased clay loading from 3 to 7%. This trend could be anticipated based on increased tortuous path for diffusing molecules. The reduction in relative permeability for different gases was observed to be different for a particular membrane. In butyl rubber/vermiculite membranes, the relative permeability for various gases differed by as much as a factor of two for a given membrane [8].

A nominal aspect ratio ( $\alpha'$ ) is usually calculated by fitting relative permeability data as the function of clay content [7,8,29–31]. From the trend obtained in the reduction in He permeability (Figs. 8 and 9),  $\alpha'$  was estimated by following Nielsen's model (Eq. (1)) developed for depicting barrier properties of composites containing platelet particles [32].

$$P_{\rm c} = P_{\rm p} \left( \frac{1 - \phi_{\rm f}}{1 + \alpha' \phi_{\rm f}/2} \right) \tag{1}$$

where  $P_c$  and  $P_p$  are the permeability of the composite medium and the pure polymer, respectively; while  $\phi_f$  is the volume fraction of the filler. Helium gas was chosen to estimate  $\alpha'$  using Eq. (2) in view of non-interacting nature of this gas. Transport of He would be diffusion controlled [10] and more accurate prediction of  $\alpha'$  could thus be possible. For nanocomposites based on 6A,  $\alpha'$ was estimated to be 33, while in case of 10A based nanocomposites, the same was found to be 51. This indicated higher level of clay dispersion in case of 10A based nanocomposites than for 6A based. This was in agreement with XRD, TEM, density and viscosity analysis of 10A and 6A based nanocomposites, which indicated better dispersion of 10A clay in the polymer matrix. As seen from Figs. 8 and 9, reduction in He permeability varied considerably than for other gases like CH<sub>4</sub> and CO<sub>2</sub>. It could be anticipated that in addition to diffusion, permeability variations of these gases could also be contributed by sorption component. Owing to this, Nielsen's model cannot be directly applied for these gases in the present case. Wang et al. [29] has reported reduction in diffusion (59.5%) as well as in calculated solubility (22.9%) for N<sub>2</sub> in rectorite/SBR composites. Ryu and Chang [9] also observed that variation in the relative permeability of O2, N2 and CO2 was different at certain MMT content in LLDPE.

According to the simple composite theory [8], tortuosity factor depends on the content of particles, their shape, location and orientation in space; however, it should not depend on absolute particle size or what the penetrant is. Variations observed in the reduction of permeability for different gases as reported in the literature [8-10] and also in the present case does not seem to support this composite theory completely. The reduction in permeability may also depend upon the size and condensability of penetrant gas molecules. The gas permeability in polymer matrix is governed by solubility (affected by condensability and membrane-penetrant interactions) as well as diffusivity (affected by size and shape of the penetrant). It could be seen from the literature reports [8,10] that both these basic properties are affected by polymer-clay nanocomposites formation. It was observed that for He, diffusion rather than solubility was responsible for the reduction in the permeability; while for N2 and O2, both diffusivity as

well as solubility were reduced by the presence of clay-fillers in PP-clay nanocomposites [10]. It was also stated that for more condensable gases, interactions along the clay-PP matrix interface may affect the gas sorption process in the polymer membrane. In the present case, gas sorption and diffusion analysis though could not be performed; an increase in packing density of polymer chains (as revealed by decrease in  $d_{\rm sp}$ ) probably affected both, solubility as well as diffusivity. Variations in packing density in the same family of polymers by structural variations is known to vary both these crucial parameters responsible for permeation [33-35]. Thus, the simple composite theory may not be sufficient to explain variations in gas permeability caused by nanocomposites formation and gas solubility need to be considered in addition to just the diffusion. Increased CO<sub>2</sub> sorption in butyl rubber-vermiculite nanocomposite [8], decreased sorption of O<sub>2</sub> and N<sub>2</sub> in PP-clay nanocomposite [10], increase in free volume for molecular transport in case of poly(1-trimethylsilyl-1-propyne) [11] and poly(4-methyl-2-pentyne) [12] could be stated as some of the optimistic examples, which indicate that with a proper selection of polymer and filler type, it may be possible to widen the difference between relative permeability variations of different gases. In other words, this can be utilized as a tool to drive selectivity of particular gas pair in a desired direc-

#### 3.4.2. Effect on selectivity

Variation in the selectivity for different gas pairs in comparison to the selectivity of pristine PA (Table 3) showed a complex trend at different 6A and 10A loading in resulting nanocomposites. The  $\alpha(\text{He/CO}_2)$  was increased up to five times; while,  $\alpha(CO_2/N_2)$  and  $\alpha(CO_2/CH_4)$  were decreased at all the loading percentages. A larger decrease in permeability of CH<sub>4</sub> than for He, particularly at 7% loading led to considerable increase in  $\alpha(\text{He/CH}_4)$ . A 2.7 times increase in  $\alpha(\text{He/O}_2)$  in PP-clay nanocomposite was reported [10]. The CO<sub>2</sub> based selectivities,  $\alpha(CO_2/N_2)$  and  $\alpha(CO_2/CH_4)$  in present case were reduced dramatically as a result of larger drop in CO<sub>2</sub> permeability (52-91%) than for either  $N_2$  or  $CH_4$  (up to 71%) for different nanocomposite membranes. This greater reduction in permeability of CO<sub>2</sub> than that of N<sub>2</sub> and CH<sub>4</sub> is an anomalous behavior. Both the contributing factors to permeability, i.e. diffusivity and/or solubility cannot be anticipated to be reduced based solely on established assumptions. Reduction in the diffusivity may not be just based on kinetic diameter of CO<sub>2</sub>, which is smaller than that of N<sub>2</sub> and CH<sub>4</sub>. Similarly, sorption of CO<sub>2</sub> in polymer matrix is usually much higher than that of N<sub>2</sub> and CH<sub>4</sub> in most of the polymeric materials. At least for the type of polymer used here (polyarylate) this is well established. There could be some other factor responsible for this observed anomaly. It was observed that for a particular case of benzoylation of PPO, reduction in gas permeability for different gases followed the order: He < CH<sub>4</sub> < N<sub>2</sub> < CO<sub>2</sub>, which was in the order of their increasing molar mass and not the kinetic diameter [36]. Thus, in addition to kinetic diameter, other properties of CO<sub>2</sub> (molar mass or cylindrical nature) may also be responsible for execution of 'diffusion jump' from one activated site to another. This issue needs more investigations and supporting evidences.

An increase in He/CH<sub>4</sub> selectivity could be seen only at 7% loading, indicating that there could be a bare minimum requirement for clay loading to affect selectivity favorably in these PA based nanocomposites. This could be possible especially in view of the presence of long alkyl chain of organic modifier of the clay. Though such modifier is required to induce compatibility of the clay with polymer chains, it is usually composed of long alkyl chains, which can also induce plasticization as observed by decrease in glass transition temperature in present case. This decrease in  $T_{\rm g}$  could be anticipated to adversely affect the selectivity performance owing to poorer penetrant-discriminating ability due to plasticization. A smaller variation in  $\alpha(\text{He/CH}_4)$  selectivity at 3–5% loading suggested that probably this plasticization effect is more predominant than the tortuous path offered at this loading level in governing selectivity, while at 7% loading, much higher tortuous path may be predominantly responsible to reduce permeability of larger gases, leading to higher selectivity of He/CO2 and He/CH<sub>4</sub> pairs. In order to tune selectivity favorably, selection of alkyl group modifier (intercalant/surfactant) that would show minimal plasticization effect and at the same time facilitate maximum possible interactions (may be exfoliation) may be required. Variation in other physical properties by nanocomposites formation that govern gas sorption and diffusion can also be crucial.

## 4. Conclusions

Polyarylate—clay nanocomposite were prepared by solution intercalation method using 6A and 10A clay. Attractive interactions were more predominant in case of 10A clay based nanocomposites than that for 6A based cases, as evidenced by higher solution viscosity and density for earlier case. TEM analysis revealed that the clay layers were dispersed at nanometer scale in the polymer matrix. Organic modifier of clay reduced glass transition temperature of formed nanocomposites as revealed by DMA analysis.

Overall decrease in permeability for all the gases was observed with incremental loading of both the types of clays. Predicted aspect ratio by Nielsen's model for both the nanocomposites was in agreement with the observed variation in physical properties of 6A and 10A based nanocomposites. Marked decrease in permeability of gases like CO<sub>2</sub> and CH<sub>4</sub>, in comparison to relatively lower decrease in permeability of He was observed, especially at higher clay loading. An increase in selectivity:  $\alpha(\text{He/CO}_2)$  and  $\alpha(\text{He/CH}_4)$ , especially at higher clay loading indicated the capability of nanocomposites to tune the selectivity favorably. A bare minimum requirement of clay loading to successfully overcome the effect of plasticization towards lowering in selectivity was noted. This indicated that if alky group modifier could be chosen such that it would minimize plasticization and facilitate clay exfoliation while inducing compatibility of clay with polymer chains, the permeation properties, especially selectivity behavior could be better tuned.

# Acknowledgements

Y.S. Bhole is thankful to the Council of Scientific and Industrial Research (India) for the Senior Research Fellowship. The authors acknowledge Mrs. Anuya Nisal for TEM micrographs and Southern Clay Products (United States) for gifting clay samples.

#### References

- K.E. Strawhecker, E. Manias, Structure and properties of poly(vinyl alcohol)/Na<sup>+</sup> montmorillonite nanocomposites, Chem. Mater. 12 (2000) 2943–2949.
- [2] R. Xu, E. Manias, A.J. Snyder, J. Runt, New biomedical poly(urethane urea)-layered silicate nanocomposites, Macromolecules 34 (2001) 337–339.
- [3] K. Yano, A. Usuki, A. Okada, T. Kurauchi, O. Kamigaito, Synthesis and properties of polyimide–clay hybrid, J. Polym. Sci., Part A: Polym. Chem. 31 (1993) 2493–2498.
- [4] P.B. Messersmith, E.P. Giannelis, Synthesis and barrier properties of poly(e-caprolactone)-layered silicate nanocomposites, J. Polym. Sci., Part A: Polym. Chem. 33 (1995) 1047–1057.
- [5] O. Khayankarn, R. Magaraphan, J.W. Schwank, Adhesion and permeability of polyimide–clay nanocomposite films for protective coatings, J. Appl. Polym. Sci. 89 (2003) 2875–2881.
- [6] J. Chang, Y.U. An, G.S. Sur, Poly(lactic acid) nanocomposites with various organoclays. I. Thermomechanical properties, morphology, and gas permeability, J. Polym. Sci., Part B: Polym. Phys. 41 (2003) 94–103.
- [7] T. Lan, P.D. Kaviratna, T.J. Pinnavaia, On the nature of polyimide–clay hybrid composites, Chem. Mater. 6 (1994) 573–575.
- [8] S. Takahashi, H.A. Goldberg, C.A. Feeney, D.P. Karim, M. Farrell, K. O'Leary, D.R. Paul, Gas barrier properties of butyl rubber/vermiculite nanocomposite coatings, Polymer 47 (2006) 3083–3093.
- [9] S.H. Ryu, Y. Chang, Factors affecting the dispersion of montmorillonite in LLDPE nanocomposite, Polym. Bull. 55 (2005) 385–392.
- [10] J.P.G. Villaluenga, M. Khayet, M.A. Lopez-Manchado, J.L. Valentin, B. Seoane, J.I. Mengual, Gas transport properties of polypropylene/clay composite membranes, Eur. Polym. J. 43 (2007) 1132–1143.
- [11] T.C. Merkel, Z. He, I. Pinnau, B.D. Freeman, P. Meakin, A.J. Hill, Effect of nanoparticles on gas sorption and transport in poly(1-trimethylsilyl-1propyne), Macromolecules 36 (2003) 6844–6855.
- [12] T.C. Merkel, B.D. Freeman, R.J. Spontak, Z. He, I. Pinnau, P. Meakin, A.J. Hill, Sorption, transport, and structural evidence for enhanced free volume in poly(4-methyl-2-pentyne)/fumed silica nanocomposite membranes, Chem. Mater. 15 (2003) 109–123.
- [13] K. Ghosal, B.D. Freeman, Gas separation using polymer membranes: an overview, Polym. Adv. Tech. 5 (1994) 673–697.
- [14] U.K. Kharul, S.S. Kulkarni, M.G. Kulkarni, A.Y. Houde, S.G. Charati, S.G. Joshi, Gas permeation in polyarylates: effect of bisphenol and acid substitution symmetry, Polymer 39 (1998) 2011–2022.
- [15] R.M. Venkateswara, A.J. Rojivadiya, P.H. Parsania, H.H. Parekh, A convenient method for the preparation of bisphenols, J. Ind. Chem. Soc. 64 (1987) 758–759.
- [16] A. Sorrentino, M. Tortora, V. Vittoria, Diffusion behavior in polymer–clay nanocomposites, J. Polym. Sci., Part B: Polym. Phys. 44 (2006) 265–274.
- [17] B. Xu, Q. Zheng, Y. Song, Y. Shangguan, Calculating barrier properties of polymer/clay nanocomposites: effects of clay layers, Polymer 47 (2006) 2904–2910.
- [18] A.B. Morgan, J.D. Harris, Effects of organoclay soxhlet extraction on mechanical properties, flammability properties and organoclay dispersion of polypropylene nanocomposites, Polymer 44 (2003) 2313–2320.
- [19] H. Acharya, S.K. Srivastava, A.K. Bhowmick, Ethylene propylene diene terpolymer/ethylene vinyl acetate/layered silicate ternary nanocomposite by solution method, Polym. Eng. Sci. 46 (2006) 837–843.
- [20] S. Hsiao, G. Liou, L. Chang, Synthesis and properties of organosoluble polyimide/clay hybrids, J. Appl. Polym. Sci. 80 (2001) 2067–2072.

- [21] A.R. Manninen, H.E. Naguib, A.V. Nawaby, M. Day, CO<sub>2</sub> sorption and diffusion in polymethyl methacrylate–clay nanocomposites, Polym. Eng. Sci. 45 (2005) 904–914.
- [22] Z. Shen, G.P. Simon, Y. Cheng, Comparison of solution intercalation and melt intercalation of polymer–clay nanocomposites, Polymer 43 (2002) 4251–4260.
- [23] L. Priya, J.P. Jog, Poly(vinylidene fluoride)/clay nanocomposites prepared by melt intercalation: crystallization and dynamic mechanical behavior studies, J. Polym. Sci., Part B: Polym. Phys. 40 (2002) 1682–1689.
- [24] R.A. Vaia, E.P. Giannelis, Polymer melt intercalation in organically-modified layered silicates: model predictions and experiment, Macromolecules 30 (1997) 8000–8009.
- [25] D. Wang, D. Parlow, Q. Yao, C.A. Wilkie, PVC–clay nanocomposites: preparation, thermal and mechanical properties, J. Vinyl Addit. Technol. 7 (2001) 203–213.
- [26] A. Wang, T.J. Pinnavaia, New directions in polymer-clay nanocomposite formation, Polym. Mater. Sci. Eng. 82 (2000) 274–275.
- [27] X. Li, T. Kang, W. Cho, J. Lee, C. Ha, Preparation and characterization of poly(butyleneterephthalate)/organoclay nanocomposites, Macromol. Rapid Commun. 22 (2001) 1306–1312.
- [28] S.S. Ray, K. Yamada, M. Okamoto, A. Ogami, K. Ueda, New polylactide/layered silicate nanocomposites. 3. High-performance biodegradable materials, Chem. Mater. 15 (2003) 1456–1465.

- [29] Z.F. Wang, B. Wang, N. Qi, H.F. Zhang, L.Q. Zhang, Influence of fillers on free volume and gas barrier properties in styrene–butadiene rubber studied by positrons, Polymer 46 (2005) 719–724.
- [30] M.A. Osman, V. Mittal, H.R. Lusti, The aspect ratio and gas permeation in polymer-layered silicate nanocomposites, Macromol. Rapid Commun. 25 (2004) 1145–1149.
- [31] S. Hotta, D.R. Paul, Nanocomposites formed from linear low density polyethylene and organoclays, Polymer 45 (2004) 7639– 7654.
- [32] L.E. Nielsen, Models for the permeability of filled polymer systems, J. Macromol. Sci. (Chem.) A1 (5) (1967) 929–942.
- [33] J.S. McHattie, W.J. Koros, D.R. Paul, Gas transport properties of polysulphones: 1. Role of symmetry of methyl group placement on bisphenol rings, Polymer 32 (1991) 840–850.
- [34] M.R. Pixton, D.R. Paul, Gas transport properties of polyarylates: substituent size and symmetry effects, Macromolecules 28 (1995) 8277– 8286
- [35] N. Muruganandam, W.J. Koros, D.R. Paul, Gas sorption and transport in substituted polycarbonates, J. Polym. Sci., Part B: Polym. Phys. 25 (1987) 1999–2026.
- [36] Y.S. Bhole, U.K. Kharul, S.P. Somani, S.C. Kumbharkar, Benzoylation of polyphenylene oxide: characterization and gas permeability investigations, Eur. Polym. J. 41 (2005) 2461–2471.